Dynamic properties of the dimerized spin-½ isotropic XY chain in a transverse field

2002 J. Phys. A: Math. Gen. 35 3573

(http://iopscience.iop.org/0305-4470/35/16/301)

INSTITUTE OF PHYSICS PUBLISHING JOURNAL OF PHYSICS A: MATHEMATICAL AND GENERAL

J. Phys. A: Math. Gen. **35** (2002) 3573–3596 PII: S0305-4470(02)29587-6

Dynamic properties of the dimerized spin-$\frac{1}{2}$ isotropic XY chain in a transverse field

Oleg Derzhko[1,2], Taras Krokhmalskii[1] and Joachim Stolze[3]

[1] Institute for Condensed Matter Physics, 1 Svientsitskii Street, L'viv-11, 79011, Ukraine
[2] Chair of Theoretical Physics, Ivan Franko National University of L'viv, 12 Drahomanov Street, L'viv-5, 79005, Ukraine
[3] Institut für Physik, Universität Dortmund, 44221 Dortmund, Germany

E-mail: derzhko@icmp.lviv.ua, krokhm@icmp.lviv.ua and stolze@physik.uni-dortmund.de

Received 5 October 2001, in final form 14 February 2002
Published 12 April 2002
Online at stacks.iop.org/JPhysA/35/3573

Abstract
The zz and xx (yy) dynamic structure factors of the dimerized spin-$\frac{1}{2}$ isotropic XY chain in a transverse (z) field are calculated for arbitrary temperatures. The zz structure factor can be given in analytical terms, involving a single integration, whereas the xx dynamic structure factor can be evaluated completely numerically for very long chains. We compare the two structure factors and discuss in some detail how a dimerization manifests itself in the dynamic structure factors at different external fields and temperatures. We compare our results to corresponding results for the dimerized Heisenberg chain obtained by approximate techniques.

PACS numbers: 75.10.−b, 02.60.−x, 05.10.−a, 05.70.Ce, 82.35.−x

1. Introduction

The dynamic properties of dimerized quantum spin chains have recently been at the focus of many studies mainly in connection with the discovery of spin-Peierls and structurally dimerized chains [1, 2]. On the one hand, neutron scattering is a basic experimental technique in the study of such compounds [3] and the interpretation of experimental data requires a corresponding theoretical background. On the other hand, theoretical studies of the dynamic properties are interesting in their own right even for uniform quantum spin chains. Moreover, the dynamics of the dimerized chain should exhibit new features, which reflect in a complicated way the regular alternation of the exchange interaction connected with a lattice distortion.

Usually, to model the quantum dimerized magnetic chain one employs the Heisenberg model (sometimes with modifications, e.g., frustration, interchain interactions etc). Unfortunately all existing theories of the dynamic properties of the latter model (see, e.g., [4–11]) involve approximations and hence it is mandatory to compare the results obtained

by various approaches in order to separate the influence of the approximation made from the generic properties of the system studied. However, some basic features of dimerized spin chains can be illustrated within the simpler framework of a spin-$\frac{1}{2}$ XY chain. By means of the Jordan–Wigner transformation that spin chain can be mapped onto a system of noninteracting spinless fermions and therefore a rigorous analysis of many statistical mechanical properties becomes possible [12]. The same reformulation in terms of the Jordan–Wigner fermions applied to the Heisenberg chain results in interacting fermions and therefore further approximations are required to proceed with the derivation of the statistical mechanical quantities.

The thermodynamic properties of the spin-$\frac{1}{2}$ XY chain in a transverse field and with modulations due to either a spin-Peierls transition or a permanent structural deformation have been analysed extensively [13–20]. The dynamic properties are more difficult to analyse; up to now research was mainly restricted to the uniform case. The z spin component at each site is expressed as a product of two Fermi operators attached to that site and therefore the zz dynamics is well understood [21, 15]. In contrast, the x or y spin components at each site are essentially nonlocal objects in terms of Jordan–Wigner fermions involving Fermi operators attached not only to that particular site but to a string of sites extending to the boundary of the system. As a result the xx (yy, xy, yx) time-dependent spin correlation functions are complicated averages of products of a large number of Fermi operators. A series of papers present the infinite temperature results [22–24]; the results at finite and zero temperatures are restricted to asymptotics and special combinations of the Hamiltonian parameters [25–30]. There were several attempts to study the xx (yy, xy) dynamics numerically [31–35]. The results obtained numerically agree with the exact analytical expressions known in some limiting cases and, as a matter of fact, constitute the only results available at finite temperatures and arbitrary Hamiltonian parameters. Our numerical approach to the dynamic properties of the spin-$\frac{1}{2}$ XY chain in a transverse field [35] is not restricted to the uniform case but can be easily applied for arbitrary nonuniform chains.

In this paper we present the first results for the zz and xx (yy) dynamic structure factors for a wide range of temperatures and transverse fields for the regularly alternating spin-$\frac{1}{2}$ isotropic XY chain in a transverse field obtained partly analytically and partly numerically. After a brief introduction to the model and explanation of the numerical approach (section 2) we present results for the time-dependent spin pair correlation functions (section 3). We validate our approach by comparing the numerical findings with the exact results for zz correlation functions and with the exact results for xx (yy) correlation functions at infinite temperature and at zero temperature in a strong transverse field. Further we present numerical results for the xx (yy) dynamic structure factor (section 4) and compare them to the corresponding results for the zz dynamics [24, 15, 36]. We compare the computed dynamic structure factors with the corresponding quantities for the Heisenberg chain as obtained from various approximations [8, 11, 37]. We conclude with a brief summary (section 5).

2. Model and method

We consider a nonuniform one-dimensional isotropic XY model in a transverse field which consists of $N \to \infty$ spins one-half governed by the Hamiltonian

$$H = \Omega \sum_{n=1}^{N} s_n^z + \sum_{n=1}^{N-1} J(1 - (-1)^n \delta) \left(s_n^x s_{n+1}^x + s_n^y s_{n+1}^y \right). \tag{1}$$

Here Ω is the magnetic field directed along the z axis (transverse field). The alternating exchange interaction $J(1 - (-1)^n \delta)$ depends on the dimerization parameter δ $(0 < \delta < 1)$,

which is a constant for a structurally dimerized chain or which is determined self-consistently by minimizing the total free energy for the spin-Peierls chain [13]. Moreover, the spin-Peierls chain exhibits the dimerized phase only for weak fields and above some characteristic value of the field a transition to an incommensurate phase occurs (see, e.g., [38]). In the limit $\delta = 0$ equation (1) corresponds to the uniform XY chain. In the opposite limit $\delta = 1$ one arrives at a collection of isolated (uncoupled) XY dimers (for a corresponding case of isolated antiferromagnetic Heisenberg dimers and applications to $KCuCl_3$ see [39]).

Our main interest is in the xx dynamic structure factor defined by

$$S_{xx}(\kappa,\omega) = \frac{1}{N}\sum_{j=1}^{N}\sum_{n=1}^{N} \mathrm{e}^{\mathrm{i}\kappa n}\int_{-\infty}^{\infty} \mathrm{d}t\, \mathrm{e}^{-\epsilon|t|}\,\mathrm{e}^{\mathrm{i}\omega t}\left\langle s_j^x(t)s_{j+n}^x\right\rangle \qquad \epsilon \to +0 \tag{2}$$

the calculation of which requires the knowledge of the time-dependent xx spin correlation functions. Because of the symmetries inherent in the model equation (2) can be rewritten as

$$\begin{aligned} S_{xx}(\kappa,\omega) = \mathrm{Re}\Bigg(\int_0^{\infty} \mathrm{d}t\, \mathrm{e}^{-\epsilon t}\,\mathrm{e}^{\mathrm{i}\omega t}\left(\left\langle s_j^x(t)s_j^x\right\rangle + \left\langle s_{j+1}^x(t)s_{j+1}^x\right\rangle + 2\cos\kappa\left(\left\langle s_j^x(t)s_{j+1}^x\right\rangle\right.\right. \\ \left.\left. + \left\langle s_{j+1}^x(t)s_{j+2}^x\right\rangle\right) + 2\cos(2\kappa)\left(\left\langle s_j^x(t)s_{j+2}^x\right\rangle + \left\langle s_{j+1}^x(t)s_{j+3}^x\right\rangle\right) + \ldots\right)\Bigg). \end{aligned} \tag{3}$$

(Note that in general $\left\langle s_j^x(t)s_{j+n}^x\right\rangle \neq \left\langle s_{j+1}^x(t)s_{j+1+n}^x\right\rangle$ due to dimerization.)

The calculation of the correlation functions $\left\langle s_j^x(t)s_{j+n}^x\right\rangle$ proceeds along the lines explained in [35]. In mapping the spin chain Hamiltonian (1) to a fermion Hamiltonian by the Jordan–Wigner transformation, the boundary conditions have to be handled with care, as already pointed out by the inventors of the XY model [12]. Boundary conditions are important since they influence the structure of the Hilbert space. It was recognized early [25] that periodic boundary conditions lead to technical problems in the calculation of dynamic x spin pair correlations which have remained unsolved until today. Therefore we have used open boundary conditions. The data we present in this paper were obtained from chains of $N = 400$ spins with $J = -1$, $\delta = 0, \ldots, 0.1, 0.2$ and the transverse field $\Omega = 0, 0.1, \ldots, 1$ at the inverse temperature $\beta = 20$ and higher temperatures. We calculated $\left\langle s_j^x(t)s_{j+n}^x\right\rangle$ in equation (3) with $j = 41$ and n up to 50 for times up to $t_c = 200$. We did the integral over t in equation (3) putting typically $\epsilon = 0.001$. We performed many test calculations similar to those described in [35] to assess the effects of finite N, j, n, t_c and ϵ for the given values of the Hamiltonian parameters and temperature. Thus we made sure that the numerical results for $S_{xx}(\kappa,\omega)$ presented in section 4 pertain to the thermodynamic limit.

We finish this section by commenting on the generalizations of our results. Making use of the transformation $s_n^{x\prime} = s_n^y$, $s_n^{y\prime} = -s_n^x$ one finds that $\left\langle s_j^y(t)s_{j+n}^y\right\rangle = \left\langle s_j^x(t)s_{j+n}^x\right\rangle$ and hence $S_{yy}(\kappa,\omega) = S_{xx}(\kappa,\omega)$. A similar transformation, $s_{2n}^{x\prime} = -s_{2n}^x$, $s_{2n}^{y\prime} = -s_{2n}^y$, shows that $\left\langle s_j^x(t)s_{j+n}^x\right\rangle$ for $J > 0$ is equal to $(-1)^n\left\langle s_j^x(t)s_{j+n}^x\right\rangle$ for $J < 0$. Thus $S_{xx}(\kappa,\omega)$ for ferromagnetic exchange interaction ($J < 0$) is equal to $S_{xx}(\pi - \kappa,\omega)$ for antiferromagnetic interaction ($J > 0$). Since the above transformation changes the sign of J but does not affect the operators s_n^z it is clear that $\left\langle s_j^z(t)s_{j+n}^z\right\rangle$ and $S_{zz}(\kappa,\omega)$ do not depend on the sign of J. Finally, knowing the dynamic structure factors $S_{\alpha\alpha}(\kappa,\omega)$ one can also examine the dynamic susceptibility $\chi_{\alpha\alpha}(\kappa,\omega)$, another quantity often used for the discussion of dynamic properties. $\mathrm{Im}\chi_{\alpha\alpha}(\kappa,\omega)$ follows from $S_{\alpha\alpha}(\kappa,\omega)$ through the fluctuation–dissipation theorem, whereas $\mathrm{Re}\chi_{\alpha\alpha}(\kappa,\omega)$ follows from $\mathrm{Im}\chi_{\alpha\alpha}(\kappa,\omega)$ through the dispersion (or Kramers–Kronig) relation [40].

3. Time-dependent pair spin correlation functions

We begin with the time-dependent zz spin correlation functions, which can be found analytically following, for example, the derivation of [15]. The Jordan–Wigner transformation [12] from spin raising and lowering operators $s_n^{\pm} = s_n^x \pm \mathrm{i}s_n^y$ to Fermi operators c_n^+, c_n is followed by the Fourier transformation $c_n = \frac{1}{\sqrt{N}}\Sigma_\kappa \exp(-\mathrm{i}\kappa n)c_\kappa$, $c_n^+ = \frac{1}{\sqrt{N}}\Sigma_\kappa \exp(\mathrm{i}\kappa n)c_\kappa^+$ with $\kappa = \frac{2\pi}{N}p$, $p = -\frac{N}{2}+1, \ldots, \frac{N}{2}$ (N is even) and finally the Bogolyubov transformation $c_\kappa = u_{\kappa+\pi}\eta_\kappa + \mathrm{i}v_\kappa\eta_{\kappa+\pi}^+$, $c_\kappa^+ = u_{\kappa+\pi}\eta_\kappa^+ - \mathrm{i}v_\kappa\eta_{\kappa+\pi}$ with

$$u_k = \frac{1}{\sqrt{2}}\sqrt{1+\frac{|\cos\kappa|}{\epsilon_\kappa}} \qquad v_\kappa = \mathrm{sgn}(\sin(2\kappa))\frac{1}{\sqrt{2}}\sqrt{1-\frac{|\cos\kappa|}{\epsilon_\kappa}}$$
$$\epsilon_\kappa = \sqrt{\cos^2\kappa + \delta^2\sin^2\kappa}. \tag{4}$$

As a result the Hamiltonian has the form $H = \sum_\kappa \Lambda_\kappa\left(\eta_\kappa^+\eta_\kappa - \frac{1}{2}\right)$ with $\Lambda_\kappa = \Omega + \lambda_\kappa$, $\lambda_\kappa = \mathrm{sgn}(\cos\kappa)J\epsilon_\kappa$. Using the relation $\langle s_j^z(t)s_{j+n}^z\rangle - \langle s_j^z\rangle\langle s_{j+n}^z\rangle = \langle c_j^+(t)c_{j+n}\rangle\langle c_j(t)c_{j+n}^+\rangle$ we derive the following expression for the time-dependent zz spin correlation functions:

$$\begin{aligned}\langle s_j^z(t)s_{j+n}^z\rangle - \langle s_j^z\rangle\langle s_{j+n}^z\rangle = \frac{1}{4\pi^2}\int_{-\pi}^{\pi}\mathrm{d}\kappa_1\,\mathrm{e}^{-\mathrm{i}\kappa_1 n}\left(\left(u_{\kappa_1}^2 - \mathrm{i}(-1)^j u_{\kappa_1}v_{\kappa_1}\right)n_{\kappa_1}\,\mathrm{e}^{\mathrm{i}\Lambda_{\kappa_1}t}\right.\\ \left. + \left(v_{\kappa_1}^2 + \mathrm{i}(-1)^j u_{\kappa_1}v_{\kappa_1}\right)n_{\kappa_1+\pi}\,\mathrm{e}^{\mathrm{i}\Lambda_{\kappa_1+\pi}t}\right)\int_{-\pi}^{\pi}\mathrm{d}\kappa_2\,\mathrm{e}^{\mathrm{i}\kappa_2 n}\left(\left(u_{\kappa_2}^2 + \mathrm{i}(-1)^j u_{\kappa_2}v_{\kappa_2}\right)\right.\\ \left.\times\left(1-n_{\kappa_2}\right)\,\mathrm{e}^{-\mathrm{i}\Lambda_{\kappa_2}t} + \left(v_{\kappa_2}^2 - \mathrm{i}(-1)^j u_{\kappa_2}v_{\kappa_2}\right)\left(1-n_{\kappa_2+\pi}\right)\,\mathrm{e}^{-\mathrm{i}\Lambda_{\kappa_2+\pi}t}\right)\end{aligned} \tag{5}$$

with the Fermi function $n_\kappa = \frac{1}{1+\mathrm{e}^{\beta\Lambda_\kappa}}$. The expression (5) possesses the $J \to -J$ symmetry mentioned above. We have used (5) to check our numerical procedures.

Explicit results are also available for the time-dependent correlations of $x\,(y)$ spin components in the infinite-temperature limit $\beta = 0$ [23, 24]. For $\beta = 0$ the correlations of the $s^x\,(s^y)$ (but not s^z) vanish at different sites. The autocorrelation functions are given by the following formulae:

$$\begin{aligned}&\langle s_j^x(t)s_j^x\rangle = \langle s_j^y(t)s_j^y\rangle = \tfrac{1}{4}\mathrm{Re}Z_j(t) \qquad \langle s_j^x(t)s_j^y\rangle = -\langle s_j^y(t)s_j^x\rangle = \tfrac{1}{4}\mathrm{Im}Z_j(t)\\ &Z_j(t) = \frac{\Theta_1\left(J_+t, \frac{J_-}{J_+}\right)}{\Theta_1\left(0, \frac{J_-}{J_+}\right)}\frac{H_1\left(J_+t, \frac{J_-}{J_+}\right)}{H_1\left(0, \frac{J_-}{J_+}\right)}\exp\left(-\mathrm{i}\Omega t - \left(1 - \frac{E\left(\frac{J_-}{J_+}\right)}{K\left(\frac{J_-}{J_+}\right)}\right)J_+^2t^2\right).\end{aligned} \tag{6}$$

Here the Jacobian theta and eta functions are defined by

$$\begin{aligned}&\Theta_1(u,k) \equiv \sum_{n=-\infty}^{\infty} q^{n^2}\,\mathrm{e}^{2niz} \qquad H_1(u,k) \equiv \sum_{n=-\infty}^{\infty} q^{\left(n+\frac{1}{2}\right)^2}\mathrm{e}^{(2n+1)\mathrm{i}z}\\ &q \equiv \exp\left(-\pi\frac{K(\sqrt{1-k^2})}{K(k)}\right) \qquad z \equiv \frac{\pi u}{2K(k)}\end{aligned} \tag{7}$$

whereas the complete elliptic integrals of first and second kinds are defined by

$$K(k) \equiv \int_0^{\frac{\pi}{2}}\frac{\mathrm{d}\theta}{\sqrt{1-k^2\sin^2\theta}} \qquad E(k) \equiv \int_0^{\frac{\pi}{2}}\mathrm{d}\theta\sqrt{1-k^2\sin^2\theta} \tag{8}$$

and $J_\pm^2 \equiv \frac{1}{4}J^2(1\pm\delta)^2$. We compared the results of our numerical computations with the analytical results at infinite temperature (6)–(8) and found excellent agreement (figure 1). From figure 1 one can see that the high-temperature limit is achieved already at $\beta = 0.1$ for

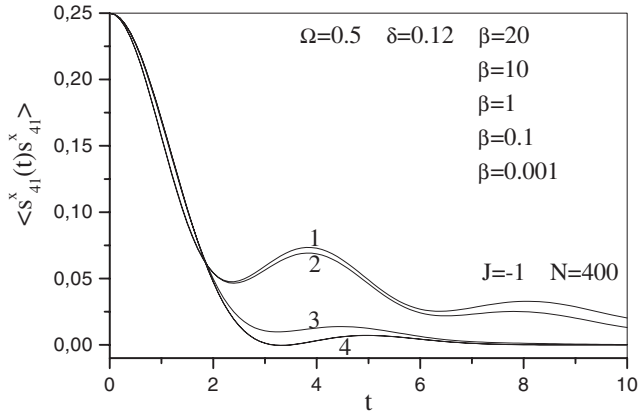

Figure 1. Time dependence of the autocorrelation function $\langle s_j^x(t)s_j^x\rangle$ obtained numerically for $j = 41$ ($J = -1$, $\Omega = 0.5$, $N = 400$, $\delta = 0.12$) for different temperatures $\beta = 20$ (1), $\beta = 10$ (2), $\beta = 1$ (3), $\beta = 0.1$ and $\beta = 0.001$ (4) (the curves for the two latter values of temperature coincide). The curve corresponding to the exact analytical result for $\beta = 0$ (6)–(8) coincides with curve 4.

the time range shown. Very small differences show up at later times, similar to the situation at $\delta = 0$ [32, 35].

One more exact result can be obtained for $\langle s_j^x(t)s_{j+n}^x\rangle$ at zero temperature $\beta = \infty$ as the value of Ω exceeds $|J|$. The ground state of the spin model is then completely polarized ($|\mathrm{GS}_s\rangle = \prod_{n=1}^{N}|\uparrow_n\rangle$ if $\Omega < -|J|$ or $|\mathrm{GS}_s\rangle = \prod_{n=1}^{N}|\downarrow_n\rangle$ if $\Omega > |J|$) or in the fermionic description completely full ($\eta_\kappa^+|\mathrm{GS}_\eta\rangle = 0$ if $\Omega < -|J|$) or completely empty ($\eta_\kappa|\mathrm{GS}_\eta\rangle = 0$ if $\Omega > |J|$). Assume, for example, that $\Omega > |J|$. Then $\langle s_j^x(t)s_{j+n}^x\rangle = \frac{1}{4}\langle \mathrm{GS}_s|s_j^-(t)s_{j+n}^+|\mathrm{GS}_s\rangle$, and further the crucial simplification occurs

$$s_m^+|\mathrm{GS}_s\rangle = \frac{1}{\sqrt{N}}\sum_\kappa \mathrm{e}^{\mathrm{i}\kappa m}(u_{\kappa+\pi}\eta_\kappa^+ - \mathrm{i}v_\kappa\eta_{\kappa+\pi}^+)|\mathrm{GS}_\eta\rangle \tag{9}$$

i.e., the Jordan–Wigner sign factor $\exp(\mathrm{i}\pi M)$ (where M is the total number of fermions at sites $l < m$) on the rhs of equation (9) yields 1 because there are no fermions in the ground state. As a result

$$\langle s_j^x(t)s_{j+n}^x\rangle = \frac{1}{4N}\sum_\kappa \mathrm{e}^{\mathrm{i}\kappa n}\left(u_\kappa^2\,\mathrm{e}^{-\mathrm{i}\Lambda_\kappa t} + v_\kappa^2\,\mathrm{e}^{-\mathrm{i}\Lambda_{\kappa+\pi}t} - \mathrm{i}(-1)^{j+n}u_\kappa v_\kappa(\mathrm{e}^{-\mathrm{i}\Lambda_\kappa t} - \mathrm{e}^{-\mathrm{i}\Lambda_{\kappa+\pi}t})\right). \tag{10}$$

In the limiting case $\delta = 0$ the rhs of equation (10) transforms into $\frac{1}{4N}\sum_\kappa \exp(\mathrm{i}(\kappa n - \Lambda_\kappa t))$, $\Lambda_\kappa = \Omega + J\cos\kappa > 0$, which yields a Bessel function [26].

In figure 2 we show time-dependent zz correlations of spins close to the centre of a chain with length $N = 800$ at zero temperature in zero magnetic field, for $\delta = 0$ (uniform) and $\delta = 0.12$ (dimerized). The dimerization-induced changes in the correlations are clearly visible but small; figure 2(b) demonstrates the breaking of translational invariance by dimerization. Comparing figure 2 to corresponding data for $\Omega = 0.1$ we observe that the correlation functions for $\delta = 0.12$ do not change on the scale of the figure, whereas those for $\delta = 0$ change slightly, in line with the fact [15] that the zero-temperature z spin dynamics is field-independent up to the threshold $\Omega = \delta$.

The xx time-dependent correlations $\langle s_j^x(t)s_{j+n}^x\rangle$ at low temperature show a stronger dependence on δ (and Ω) than their zz counterparts, as seen in figures 3 and 4. Figure 3 shows how all correlations for distances $n = 0, 1, 2$ develop similar oscillations (of increasing

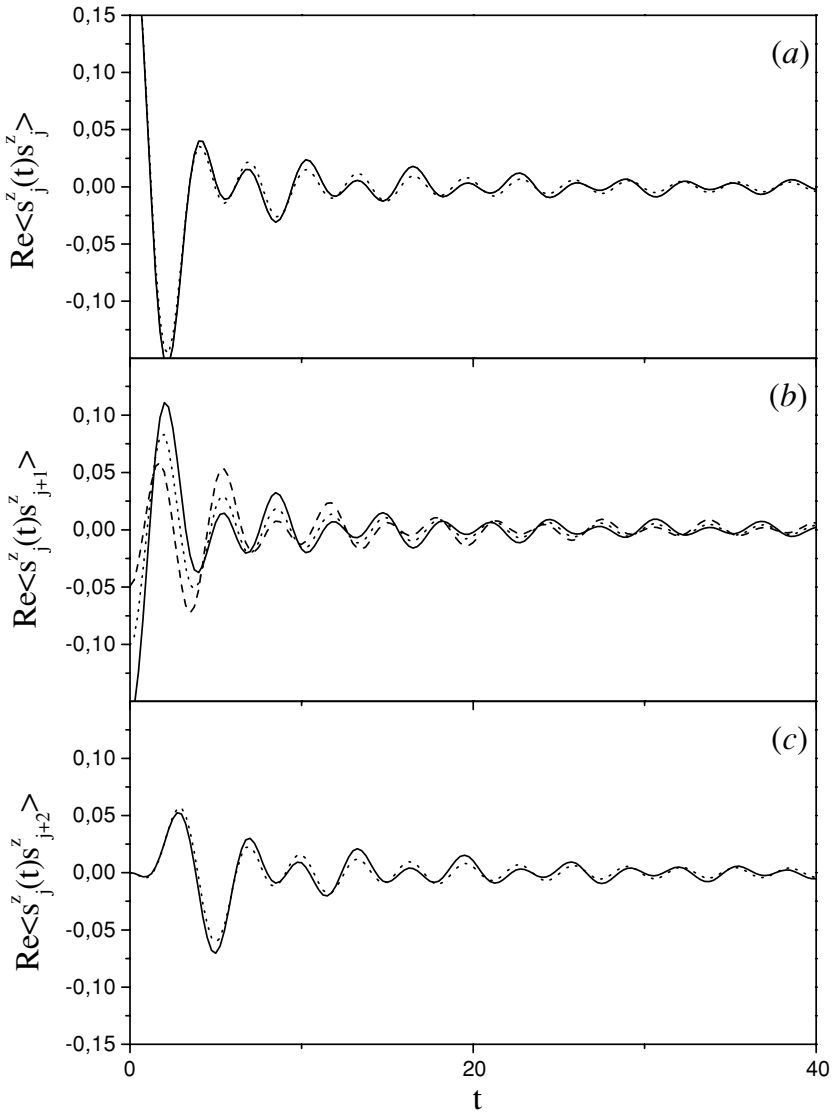

Figure 2. Real part of the correlation functions $\langle s_j^z(t)s_{j+n}^z\rangle$ at zero temperature and zero magnetic field for uniform ($\delta = 0$, dotted curves) and dimerized ($\delta = 0.12$, solid or dashed curves) $N = 800$ chains. Both $j = 401$ and $j = 402$ results are shown. For $n = 0$ (*a*) and $n = 2$ (*c*) correlations for the two j values coincide, for $n = 1$ (*b*) and $\delta = 0.12$ they split. (The solid line is for $j = 401$, the dashed line for $j = 402$.) Large j values were used in order to avoid finite-size effects which are strongest at zero temperature.

frequency) as δ grows. Figure 4 shows data for $\delta = 0$ and $\delta = 0.08$ at sites $j = 41, 42$ and for distances $n \leqslant 5$. These data demonstrate how dimerization dominates the long-time behaviour of the dynamic correlations in the sense that all correlations organize themselves into two groups according to the number of 'weak' bonds (of strength $J(1 - \delta)$) between the two sites involved. Apart from small deviations the correlations depend only on the evenness/oddness of the number of weak bonds. Analogous data for $\Omega = 0.1$ show that

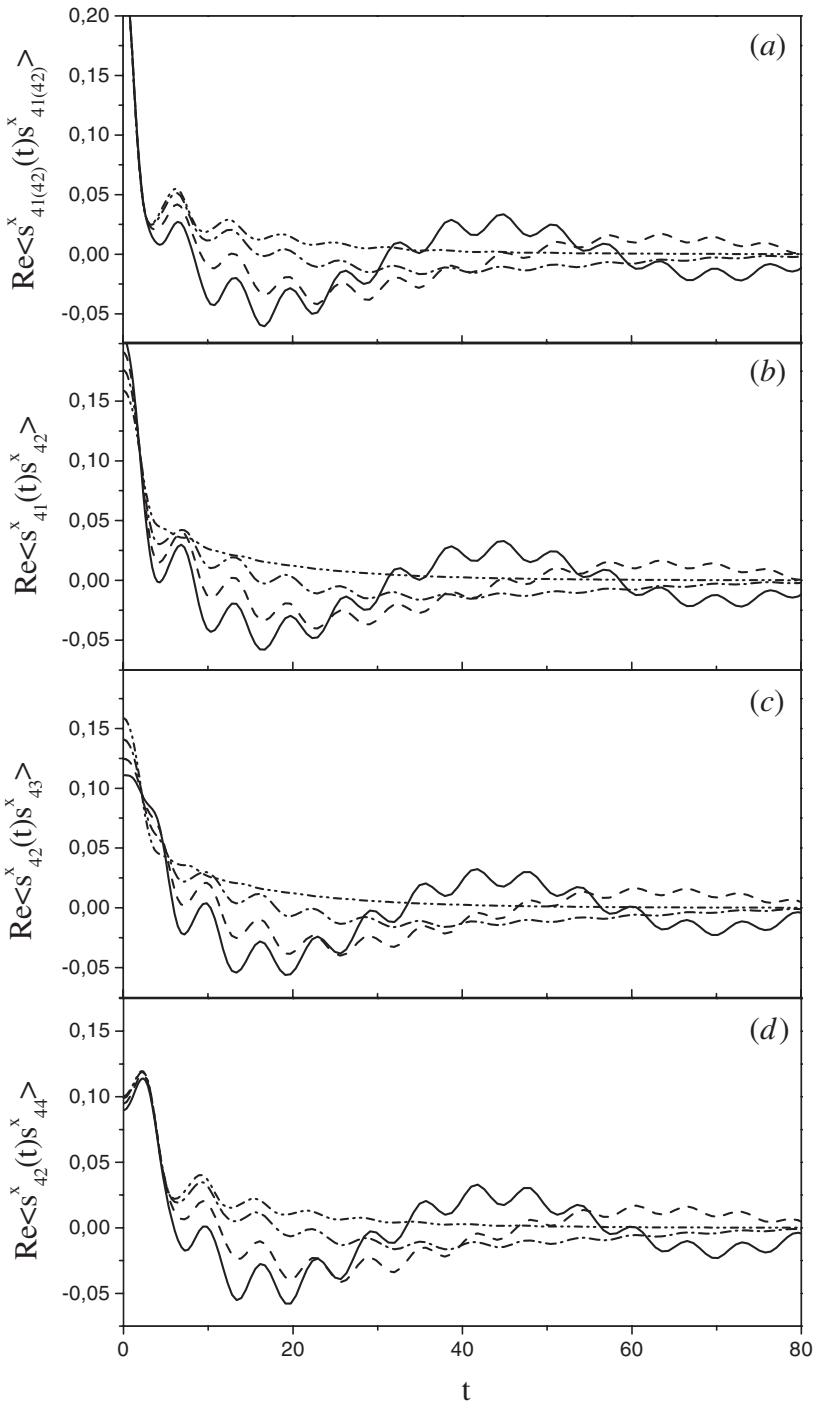

Figure 3. Real part of the correlation functions $\langle s^x_j(t)s^x_{j+n}\rangle$ at low temperature, $\beta = 20$, and small magnetic field, $\Omega = 0.000\,01$, for a $N = 400$ chain and different values of the dimerization: $\delta = 0$ (dot–dot–dashed), $\delta = 0.04$ (dot–dashed), $\delta = 0.08$ (dashed), and $\delta = 0.12$ (solid). Results for $j = 41$ and $j = 42$ are shown. These two sets of results coincide for $n = 0$ (a) and $n = 2$ (d), but they differ for $n = 1$ (b, c).

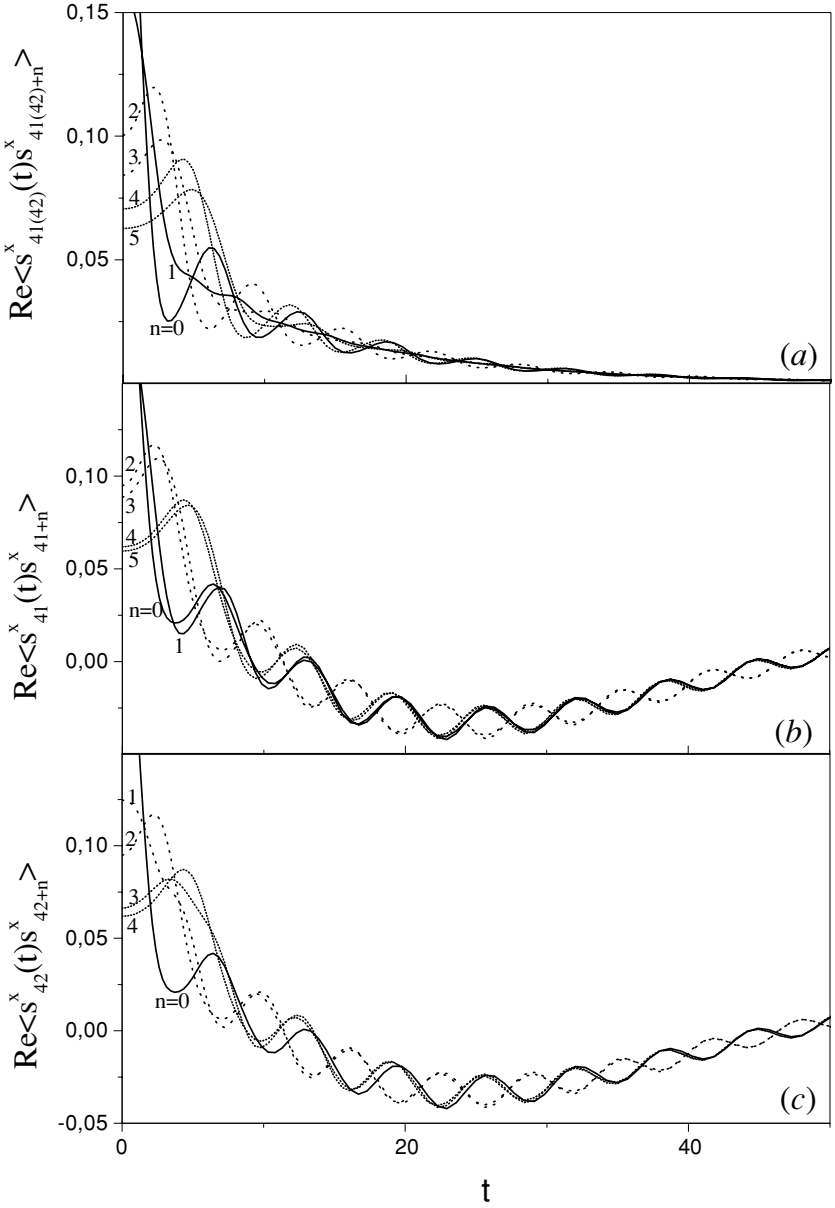

Figure 4. Real part of the correlation functions $\langle s_j^x(t)s_{j+n}^x\rangle$ at low temperature, $\beta = 20$, and small magnetic field, $\Omega = 0.000\,01$, for $N = 400$ chain and dimerizations $\delta = 0$ (*a*) and $\delta = 0.08$ (*b*), (*c*). Results for $j = 41$, 42 and various n (as denoted next to the curves) are shown. For $\delta = 0$ the results for $j = 41$ and 42 coincide. For $\delta = 0.08$ the correlation functions at long times organize into two groups according to whether the number of 'weak' ($J(1-\delta)$) bonds between the two sites is even or odd.

the magnetic field generally tends to suppress the time-dependent features introduced by the dimerization in the zero-field case. The long-time behaviour is again determined by the number of weak bonds.

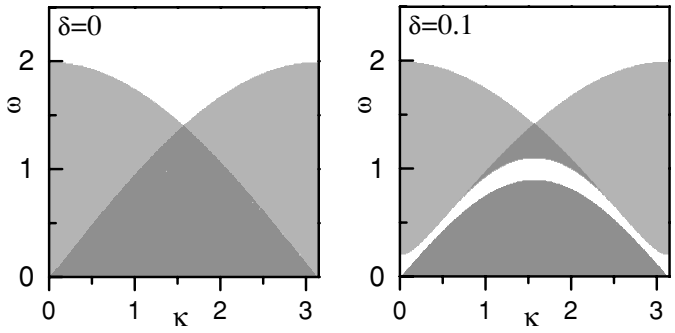

Figure 5. Location of the roots of equation (13) in the (κ, ω) plane for $\delta = 0$ and 0.1: light region: no roots, light grey region: two roots, dark grey: four roots.

4. Dynamic structure factors

In this section we discuss the dynamic structure factors $S_{zz}(\kappa, \omega)$ and $S_{xx}(\kappa, \omega)$ at low, intermediate and high temperatures.

From equation (5) the following expression for $S_{zz}(\kappa, \omega)$ may be derived[4]:

$$\begin{aligned} S_{zz}(\kappa,\omega) &= \int_{-\infty}^{\infty} \mathrm{d}t\, \mathrm{e}^{\mathrm{i}\omega t} \frac{1}{N} \sum_{j=1}^{N}\sum_{l=1}^{N} \mathrm{e}^{\mathrm{i}\kappa(l-j)} \left(\left\langle s_j^z(t) s_l^z \right\rangle - \left\langle s_j^z \right\rangle \left\langle s_l^z \right\rangle \right) \\ &= \int_{-\pi}^{\pi} \mathrm{d}\kappa' \left((u_{\kappa'} u_{\kappa'-\kappa} + v_{\kappa'} v_{\kappa'-\kappa})^2 n_{\kappa'} (1 - n_{\kappa'-\kappa})\, \delta(\omega + \lambda_{\kappa'} - \lambda_{\kappa'-\kappa}) \right. \\ &\quad \left. + (u_{\kappa'} v_{\kappa'-\kappa} - u_{\kappa'-\kappa} v_{\kappa'})^2 n_{\kappa'} (1 - n_{\kappa'-\kappa+\pi})\, \delta(\omega + \lambda_{\kappa'} - \lambda_{\kappa'-\kappa+\pi}) \right). \end{aligned} \tag{11}$$

For $\beta = \infty$ the κ' integral may be evaluated explicitly, as discussed by Taylor and Müller [15].

A closed-form expression for $S_{xx}(\kappa, \omega)$ may be obtained from equation (10) for the special case $\beta = \infty$, $\Omega > |J|$:

$$S_{xx}(\kappa,\omega) = \frac{\pi}{2} \left(u_\kappa^2 \delta(\omega - \Lambda_\kappa) + v_\kappa^2 \delta(\omega - \Lambda_{\kappa+\pi}) \right). \tag{12}$$

The basic features of $S_{zz}(\kappa, \omega)$ (11) can be interpreted in terms of the Jordan–Wigner fermions whose one-particle eigenvalues λ_κ and corresponding eigenstates are completely determined by the value of δ (for given J). Temperature and magnetic field enter only through the Fermi functions describing the thermal occupation of the eigenstates, where the magnetic field corresponds to the chemical potential. The most important variations in $S_{zz}(\kappa, \omega)$ occur along certain lines $\omega = \epsilon_i(\kappa)$ in the (κ, ω) plane which were determined and discussed in detail by Taylor and Müller [15]. (We have collected the corresponding formulae in an appendix for easy reference.)

Energy conservation implies that $S_{zz}(\kappa, \omega)$ may only differ from zero if there is a κ' ($|\kappa'| \leqslant \pi$) such that one of the two relations

$$\omega = -\lambda_{\kappa'} + \lambda_{\kappa'-\kappa} \qquad \omega = -\lambda_{\kappa'} + \lambda_{\kappa'-\kappa+\pi} \tag{13}$$

holds. Each of these two conditions can only be satisfied in a restricted region of the (κ, ω) plane; the number of corresponding κ' values is even due to the symmetries of the dispersion relation λ_κ. These regions (for positive ω) are shown in figure 5 for $\delta = 0$ and $\delta = 0.1$.

[4] The closely related dynamic susceptibility $\chi_{zz}(\kappa, \omega)$ for a more general XY chain with modulated couplings is discussed in [41].

For $\delta > 0$ there is a lower continuum of (κ, ω) points, symmetric with respect to the line $\kappa = \frac{\pi}{2}$, and two partly overlapping upper continua which are mirror images of each other. The lower continuum is bounded by the function $\epsilon_5(\kappa)$ (see appendix) and each of its points represents four possible κ' values in (11). The upper continua are bounded by $\epsilon_1(\kappa)$ and $\epsilon_2(\kappa) = \epsilon_1(\pi - \kappa)$; their common lower boundary around $\kappa = \frac{\pi}{2}$ is $\epsilon_0(\kappa)$. For $\delta \to 0$ the gap between the lower and upper continua disappears and the continua merge, as shown in the upper part of figure 5.

The distribution of spectral weight within the continua is determined by several factors. First of all, the two energy conservation δ-functions in (11) each give rise to a factor $A^{-1}(\kappa, \omega)$ where

$$A_1(\kappa, \omega) = \left| \frac{\mathrm{d}\lambda_{\kappa'}}{\mathrm{d}\kappa'} - \frac{\mathrm{d}\lambda_{\kappa'-\kappa}}{\mathrm{d}\kappa'} \right| \qquad A_2(\kappa, \omega) = \left| \frac{\mathrm{d}\lambda_{\kappa'}}{\mathrm{d}\kappa'} - \frac{\mathrm{d}\lambda_{\kappa'-\kappa+\pi}}{\mathrm{d}\kappa'} \right| \tag{14}$$

(with κ' from (13)) which may be interpreted as density-of-states factors. The zeros of $A(\kappa, \omega)$ are located at the continuum boundaries and determine potential singularities of $S_{zz}(\kappa, \omega)$. As usual in one dimension these singularities are of inverse square-root type. The Bogolyubov transformation factors enter $S_{zz}(\kappa, \omega)$ as

$$B_1(\kappa, \omega) = (u_{\kappa'} u_{\kappa'-\kappa} + v_{\kappa'} v_{\kappa'-\kappa})^2 \qquad B_2(\kappa, \omega) = (u_{\kappa'} v_{\kappa'-\kappa} - u_{\kappa'-\kappa} v_{\kappa'})^2 \tag{15}$$

(with κ' from (13)). As mentioned above, the dependence of $S_{zz}(\kappa, \omega)$ on field and temperature comes in only through the two weight factors

$$C_1(\kappa, \omega) = n_{\kappa'}(1 - n_{\kappa'-\kappa}) \qquad C_2(\kappa, \omega) = n_{\kappa'}(1 - n_{\kappa'-\kappa+\pi}) \tag{16}$$

(with κ' from (13)) which may vary between 0 and 1; for infinite temperature ($\beta = 0$) they are equal to $\frac{1}{4}$ and $S_{zz}(\kappa, \omega)$ becomes field-independent. This is apparent in the corresponding panels of figures 6 and 7.

At zero temperature the discontinuities in the weight factors (16) lead to discontinuities in $S_{zz}(\kappa, \omega)$ which become relevant for $\Omega > \delta$. As discussed in detail in [15], these discontinuities occur along lines $\epsilon_1'(\kappa)$ and $\epsilon_2'(\kappa) = \epsilon_1'(\pi - \kappa)$ within the upper continuum and along lines $\epsilon_3(\kappa)$ and $\epsilon_4(\kappa) = \epsilon_3(\pi - \kappa)$ within the lower continuum. For $\Omega < \delta$, $S_{zz}(\kappa, \omega)$ vanishes everywhere in the lower continuum, and the excitation spectrum has a gap (see figure 8). At $\Omega = \delta$, $S_{zz}(\kappa, \omega)$ begins to differ from zero along the line $\epsilon_3(\kappa)$ ($= \epsilon_4(\kappa)$); the gap in the excitation spectrum closes discontinuously (see figure 9). For larger fields $\epsilon_3(\kappa)$ and $\epsilon_4(\kappa)$ coincide no longer and a larger part of the lower continuum becomes visible in figure 10 (see also figure 9). As $\Omega \to 1$ the region where $S_{zz}(\kappa, \omega) \neq 0$ shrinks again, degenerating to the line $\epsilon_3(\kappa)$ ($= \epsilon_4(\kappa)$), and finally for $\Omega > 1$, $S_{zz}(\kappa, \omega)$ vanishes because the ground state is completely polarized.

Figures 9 and 10 also show the variations in the zero-temperature structure factor $S_{zz}(\kappa, \omega)$ in the upper continua as Ω is varied. In these continua $S_{zz}(\kappa, \omega) \neq 0$ everywhere for $\Omega < \delta$. For $\Omega > \delta$ discontinuities along the lines $\epsilon_1'(\kappa)$ and $\epsilon_2'(\kappa) = \epsilon_1'(\pi - \kappa)$ appear. The region where $S_{zz}(\kappa, \omega) \neq 0$ shrinks with growing field, first symmetrically at the lower left and right corners of the continuum, later also in the upper centre. Finally, for $\Omega \to 1$ that region degenerates to the line $\epsilon_1'(\kappa)$ ($= \epsilon_2'(\kappa)$), and for $\Omega > 1$, $S_{zz}(\kappa, \omega)$ vanishes everywhere. It is interesting to note that for $\Omega = 1^+$ the exact δ-function expression (12) for $S_{xx}(\kappa, \omega)$ takes over exactly where $S_{zz}(\kappa, \omega)$ fades away at $\Omega = 1^-$. This shows that due to the fully polarized ground state at $\Omega \geqslant 1$ both $S_{zz}(\kappa, \omega)$ and $S_{xx}(\kappa, \omega)$ rely on the same set of simple (two-particle) excitations, but with vastly different spectral weights. While $S_{xx}(\kappa, \omega)$ is a δ-function for $\Omega > 1$, $S_{zz}(\kappa, \omega)$ degenerates to a function of finite height and zero width as $\Omega \to 1$.

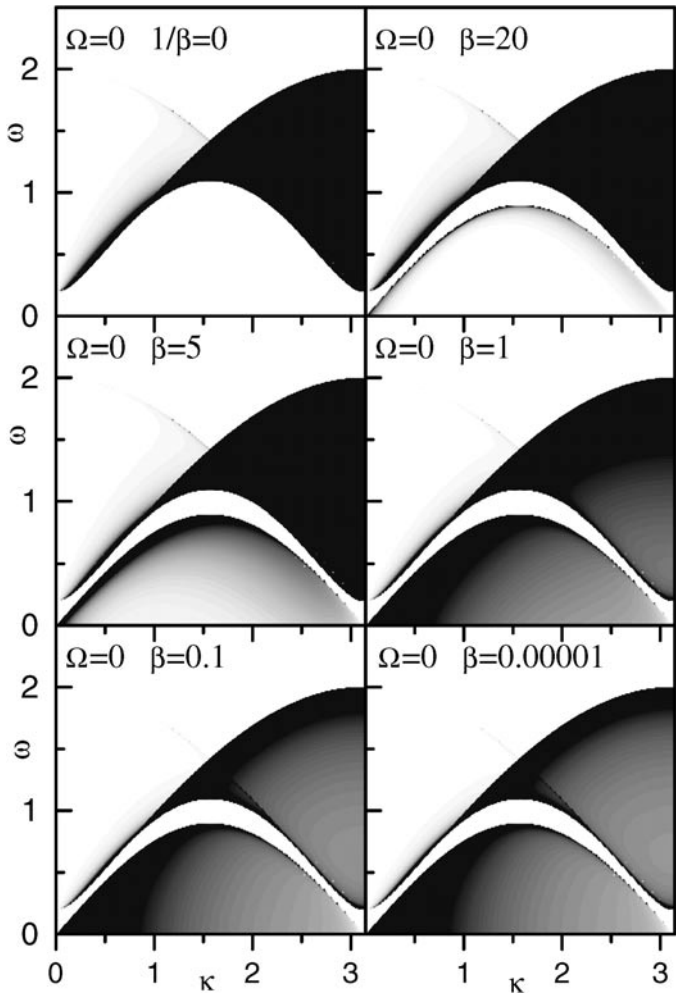

Figure 6. $S_{zz}(\kappa, \omega)$ as follows from the exact formula (11) for the spin chain (1) with $J = -1$, $\delta = 0.1$, $\Omega = 0$ at different temperatures $\beta = \infty$, 20, 5, 1, 0.1, 0.000 01.

Figures 6 and 7 show the temperature dependence of $S_{zz}(\kappa, \omega)$ at $\delta = 0.1$ for zero field and for intermediate field ($\Omega = 0.5$), respectively. The effects observed can be interpreted as variations in the occupation factors (16) whose zero-temperature discontinuities are shifted by Ω and softened by nonzero temperatures. At nonzero temperature $\beta < \infty$ the lower continuum starts to contribute to $S_{zz}(\kappa, \omega)$ for fields below the 'lower critical field' $\Omega = \delta$. With rising temperature the 'upper critical field' $\Omega = 1$ also gradually loses its importance, and the intensity redistributes within the continua. Finally all field-dependent features in $S_{zz}(\kappa, \omega)$ (such as Fermi function induced discontinuities within the continua) melt away and only the continuum boundaries remain for $\beta \to 0$. Note, however, that the distribution of spectral weight over the continua remains asymmetric up to the highest temperatures due to the temperature-independent factors $A(\kappa, \omega)$ (14) and $B(\kappa, \omega)$ (15).

In figure 11 we show the temperature-dependent redistribution of spectral weight within $S_{zz}(\kappa, \omega)$ in the extreme case $\Omega = 1$. The two scans at $\omega = 0.5$ and $\kappa = \frac{\pi}{4}$, respectively, show

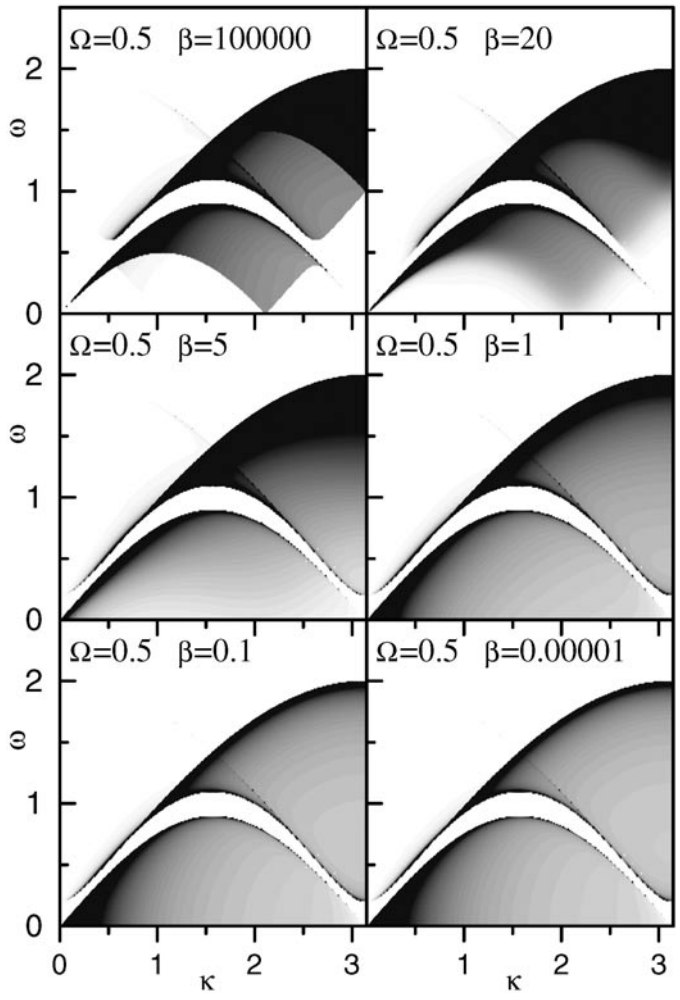

Figure 7. The same as in figure 6 for $\Omega = 0.5$.

the single peak of finite height and infinitesimally small width at zero temperature developing gradually into the continua determined by equation (13) and shown in figure 5, with their inverse square-root boundary singularities.

In figure 12 we display $S_{zz}(\kappa, \omega)$ at low temperature ($\beta = 20$) for dimerization $\delta = 0.1$ at different values of the transverse field. Analogous plots for $S_{xx}(\kappa, \omega)$ are shown in figure 13, and for high temperature ($\beta = 1$) in figure 14. The detailed comparison of these data which follows below shows that the two-particle excitation continua which determine the zz dynamic structure factor completely also dominate[5] the behaviour of the xx dynamic structure factor. This generalizes our earlier observations for the uniform chain ($\delta = 0$) [35]. However, due to the many-body nature of the x correlation function the low-temperature xx dynamic structure factor exhibits also nonzero (but small) values outside the two-particle excitation continua, again, similar to the uniform case [35]. The first panel of figure 12 shows the strong upper

[5] The importance of the two-particle excitations for the xx structure factor was already stressed by Taylor and Müller [15]; see the discussion on p 16 of that reference and the references cited there.

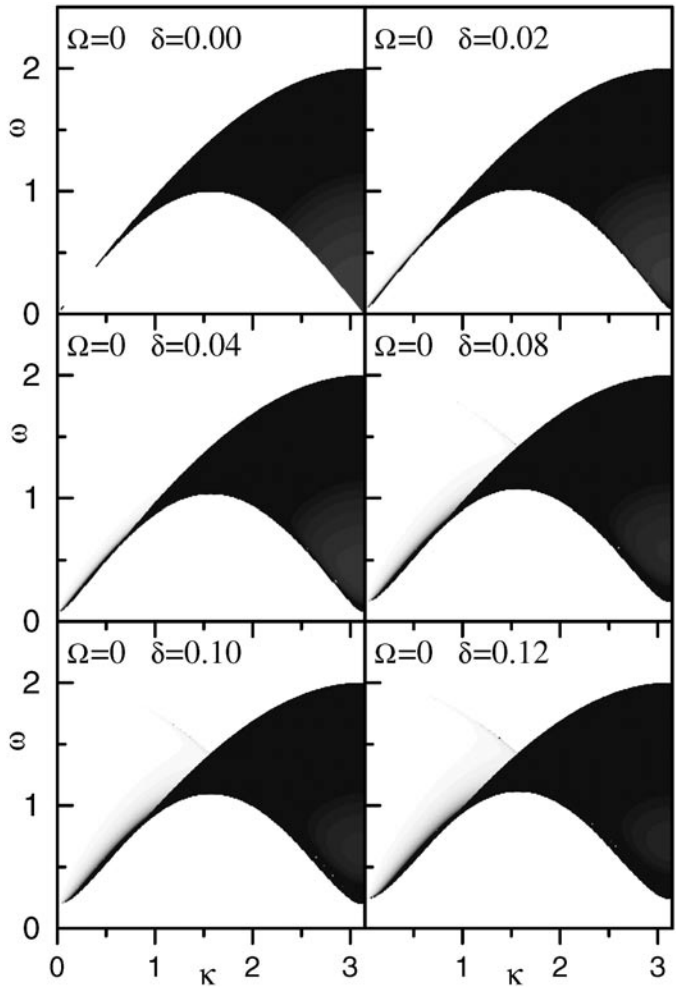

Figure 8. $S_{zz}(\kappa, \omega)$ as follows from the exact formula (11) for the spin chain (1) with $J = -1$ for different values of the dimerization parameter $\delta = 0$, 0.02, 0.04, 0.08, 0.1, 0.12 and $\Omega = 0$ at $\beta = \infty$.

excitation continuum and the emerging lower continuum in $S_{zz}(\kappa, \omega)$. Note that Ω is just at the critical value so that at zero temperature the lower continuum is still absent (compare the first panel of figure 10). Thus the emerging lower continuum is a rather strong finite-temperature effect, assisted, of course, by the diverging density of states at the upper boundary of the lower continuum. The x spin pair correlation under the Jordan–Wigner transformation corresponds to a many-body correlation, while the z correlation maps to a simple two-particle correlation, which restricts the structure factor $S_{zz}(\kappa, \omega)$ to a finite part of the (κ, ω) plane as discussed above. No such restriction applies to $S_{xx}(\kappa, \omega)$ so that one might expect nonzero values of that structure factor far above the continua displayed in $S_{zz}(\kappa, \omega)$. The opposite is true, as the first panel of figure 13 shows: $S_{xx}(\kappa, \omega)$ is rather small, except for two quite well-defined excitation branches following the lower boundary of the upper continuum and the upper boundary of the lower continuum, respectively. The frequency bandwidth of $S_{xx}(\kappa, \omega)$ thus is much smaller than that of $S_{zz}(\kappa, \omega)$ (except for small k) and not larger as naively expected. Similar tendencies

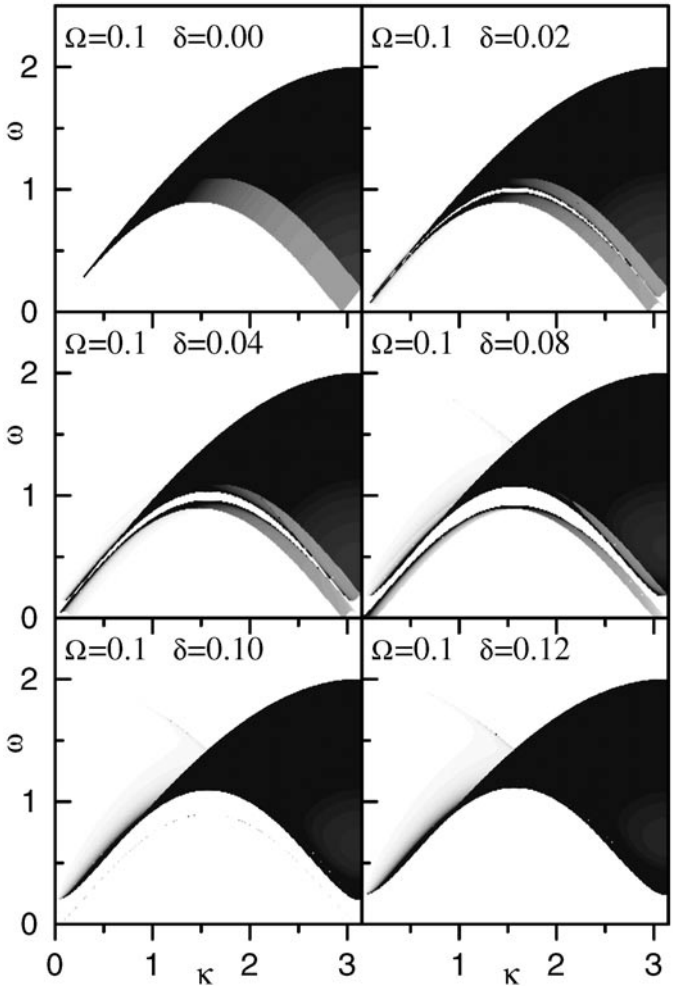

Figure 9. The same as in figure 8 for $\Omega = 0.1$.

were observed in the uniform chain [35]. Evidently this effect—reduction of a continuum to a small number of relatively well-defined modes—is a consequence of the many-body nature of the correlation function, but the detailed mechanism is still subject to speculation. At high temperature (figure 14) $S_{xx}(\kappa, \omega)$ still remains basically restricted to a finite ω band but the low-temperature structure gets lost along the way to complete κ-independence at infinite temperature. (Compare our earlier paper [35] for some high-temperature figures at $\delta = 0$.)

At higher magnetic fields (compare, for example, the $\Omega = 0.25$ panels of figures 12 and 13) the excitation branches of $S_{xx}(\kappa, \omega)$ (at low temperature) wander into the excitation continua of $S_{zz}(\kappa, \omega)$, that is, the upper branch moves upward in frequency, and the lower branch moves downward. In addition, another high-frequency branch becomes more clearly visible of which only very faint indications are present at $\Omega = 0.1$. This high-frequency excitation follows the upper boundary of the upper continuum and thus does not depend on the magnetic field. An additional low-energy branch ending at $\kappa = \pi$ starts to show up at $\Omega = 0.4$. The two low-energy branches seem to meet at a soft-mode point on the κ axis.

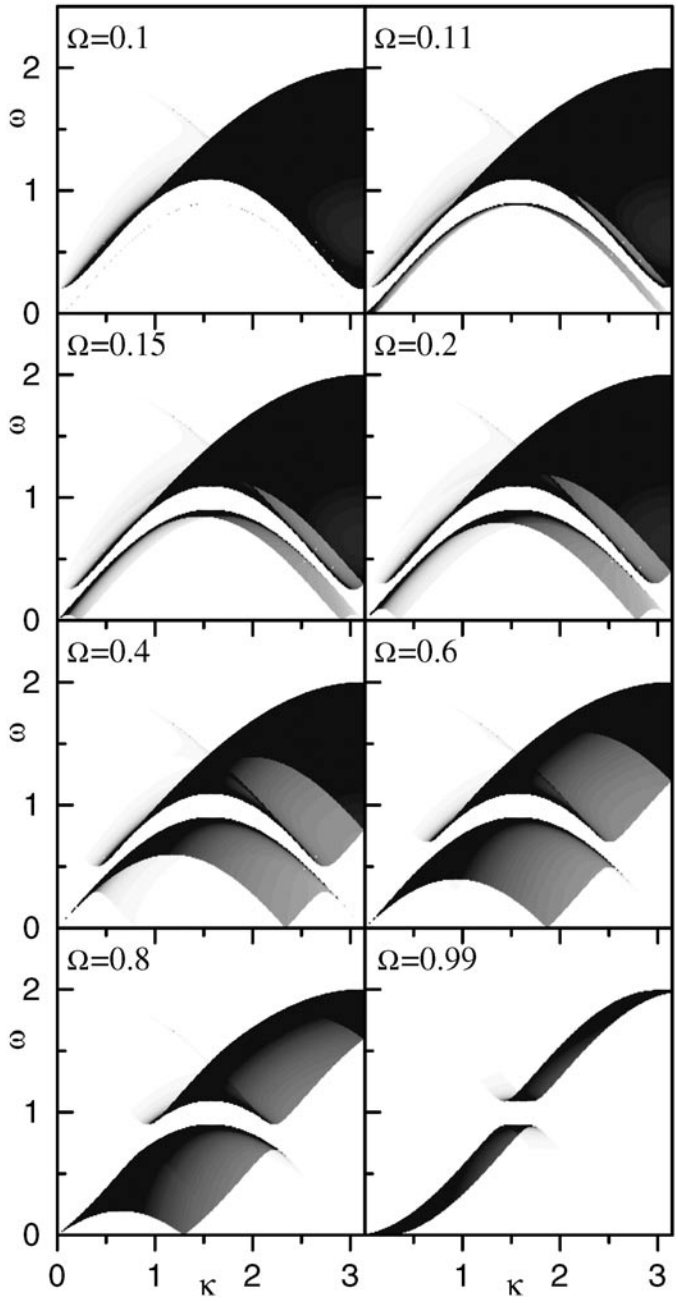

Figure 10. $S_{zz}(\kappa, \omega)$ as follows from the exact formula (11) for the spin chain (1) with $J = -1$, $\delta = 0.1$ for different values of the transverse field $\Omega = 0.1, 0.11, 0.15, 0.2, 0.4, 0.6, 0.8, 0.99$ at $\beta = \infty$. Note that $S_{zz}(\kappa, \omega)$ does not depend on Ω for $\Omega < \delta$.

Comparisons with the $\Omega = 0.4$, 0.6, and 0.8 panels of figure 10 show that these low-frequency modes of $S_{xx}(\kappa, \omega)$ coincide with the field-dependent lower boundaries of the continua of $S_{zz}(\kappa, \omega)$ at zero temperature. In the field regime where $S_{xx}(\kappa, \omega)$ displays the richest branch

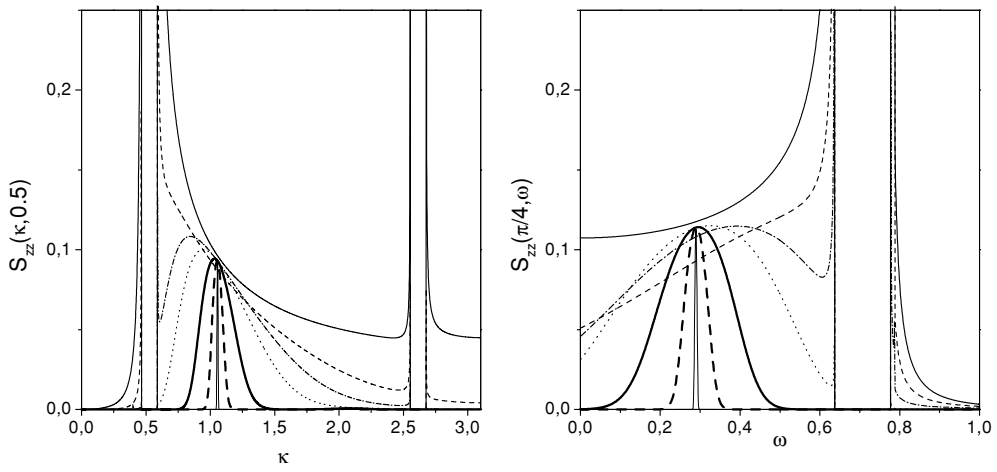

Figure 11. Constant frequency and wave vector scans of $S_{zz}(\kappa, \omega)$ (11) for the spin chain (1) with $J = -1$, $\delta = 0.1$ at the critical field $\Omega = 1$ while temperature varies ($\beta = 100\,000$ (thin solid curves), $\beta = 1000$ (thick dashed curves), $\beta = 100$ (thick solid curves), $\beta = 20$ (dotted curves), $\beta = 10$ (dot–dashed curves), $\beta = 5$ (dashed curves), $\beta = 0$ (solid curves)).

structure, that is, $0.5 \leqslant \Omega \leqslant 0.75$ we can identify these branches with those determined in [15] for zero temperature as follows. For small κ and ω there is a large accumulation of spectral weight which cannot be associated unambiguously with the many branches present in that region. Probably there is a splitting between the three branches starting at $\omega = 0$ and the one ($\epsilon_1(\kappa)$) starting at $\omega = 2\delta$. At larger κ this large accumulation of spectral weight splits into two branches. The lower branch can be identified with $\epsilon_4(\kappa)$. $\epsilon_4(\kappa)$ bends down and touches the κ axis at a soft mode and then rises again. In the vicinity of the soft mode $S_{xx}(\kappa, \omega)$ has negligible spectral weight. Beyond the soft mode κ, $S_{xx}(\kappa, \omega)$ picks up spectral weight again, up to the maximum of the right branch of $\epsilon_4(\kappa)$. From there, the lower branch of $S_{xx}(\kappa, \omega)$ (after a little gap) continues along $\epsilon_2'(\kappa)$. (Note that $\epsilon_4(\kappa)$ and $\epsilon_2'(\kappa)$ show a crossing as $\delta \to 0$.) The upper branch also is separated by a dimerization-induced gap from the small-κ and small-ω region of high spectral weight. It follows the branches $\epsilon_1(\kappa)$ and $\epsilon_1'(\kappa)$ in the region where $\epsilon_1'(\kappa)$ is an increasing function of κ. (Note that the decreasing part of $\epsilon_1'(\kappa)$ also leaves a slight trace in $S_{xx}(\kappa, \omega)$.) For large κ, the upper branch in $S_{xx}(\kappa, \omega)$ separates again, as do $\epsilon_1(\kappa)$ and $\epsilon_1'(\kappa)$, and $\epsilon_1'(\kappa)$ at $\kappa = \pi$ encounters the lower branch again.

We have thus seen that the basic spectral features of $S_{xx}(\kappa, \omega)$ at low temperature can be identified with features governing [15] the zero-temperature $S_{zz}(\kappa, \omega)$. That component of the structure factor is a simple two-particle correlation in terms of Jordan–Wigner fermions and the spectral features discussed in [15] correspond to either absolute boundaries of the two-particle excitation spectrum or magnetic-field-dependent Fermi function discontinuities (compare (16)). It is not at all clear why these two-particle features should dominate the many-body correlation $S_{xx}(\kappa, \omega)$, but, as we have observed in our numerical results, they do so. Further research is necessary to clarify this issue.

It should be noted that the dynamic structure factors of quantum spin chains can often be obtained approximately using a bosonization treatment [4, 42]. However, since that approach is restricted to low-energy physics the high-frequency branches seen in figure 13 cannot be observed within that theory.

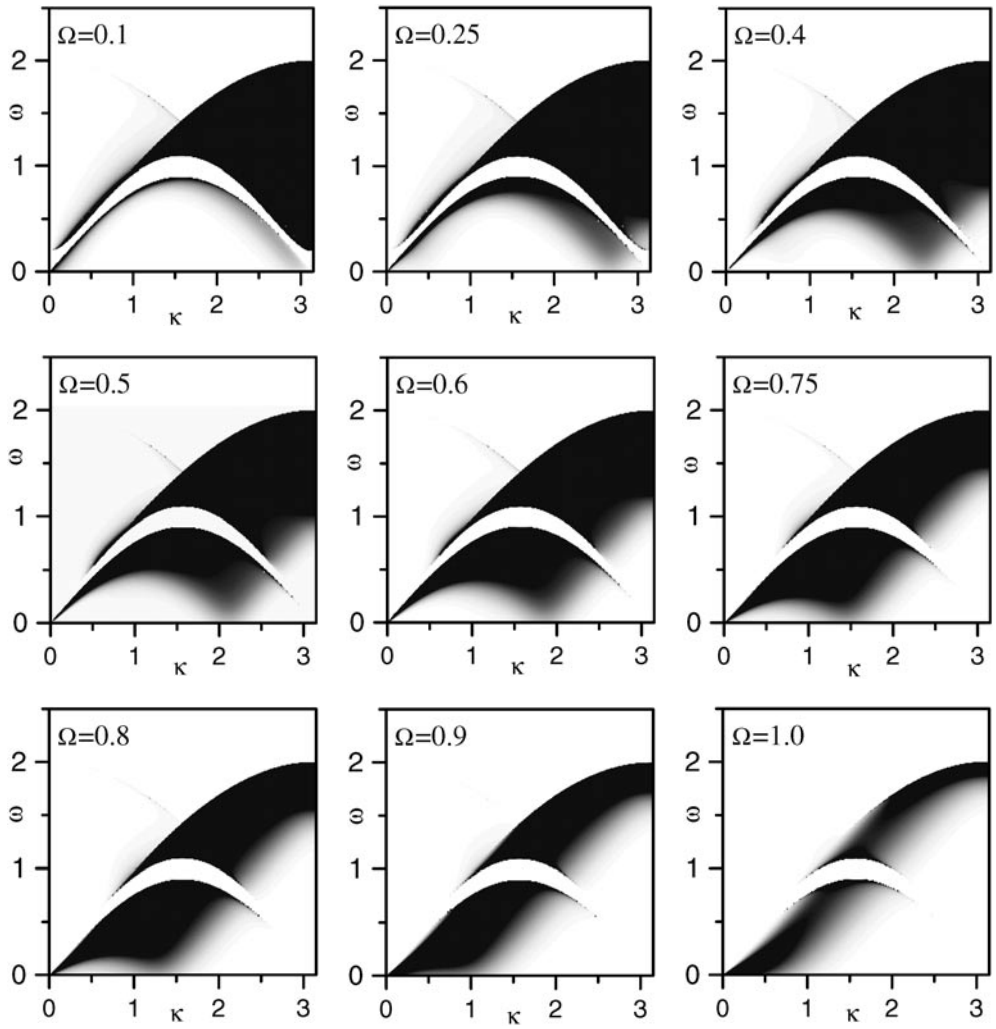

Figure 12. $S_{zz}(\kappa, \omega)$ as follows from exact formula (11) for the spin chain (1) with $J = -1$, $\delta = 0.1$ for different values of the transverse field $\Omega = 0.1, 0.25, 0.4, 0.5, 0.6, 0.75, 0.8, 0.9, 1$ at low temperature, $\beta = 20$.

Clearly, the Hamiltonian of the isotropic XY chain in a transverse field models a very special type of structurally dimerized quantum spin chain. However, combining the Hartree–Fock approximation with the Jordan–Wigner fermionization one can analyse in a similar manner the dynamic properties of the Heisenberg chain [11] (see also section 11–20 of [7] and references cited there). Without elaborating that possibility further, we finish this section by contrasting the dynamic properties of the dimerized XY chain with those of the dimerized Heisenberg chain [8, 11, 37] and with the experimental data [3] in the spin-Peierls phase of $CuGeO_3$. The theoretical results for the dimerized Heisenberg chain were obtained within the continuum approximation [8], RPA [8], the Hartree–Fock treatment [11] and exact diagonalization techniques [37]; the results reported in [37] refer to the chain in an external field. Those calculations deal with $S_{zz}(\kappa, \omega)$ ($S_{zz}(\kappa, \omega) = S_{xx}(\kappa, \omega) = S_{yy}(\kappa, \omega)$ for the

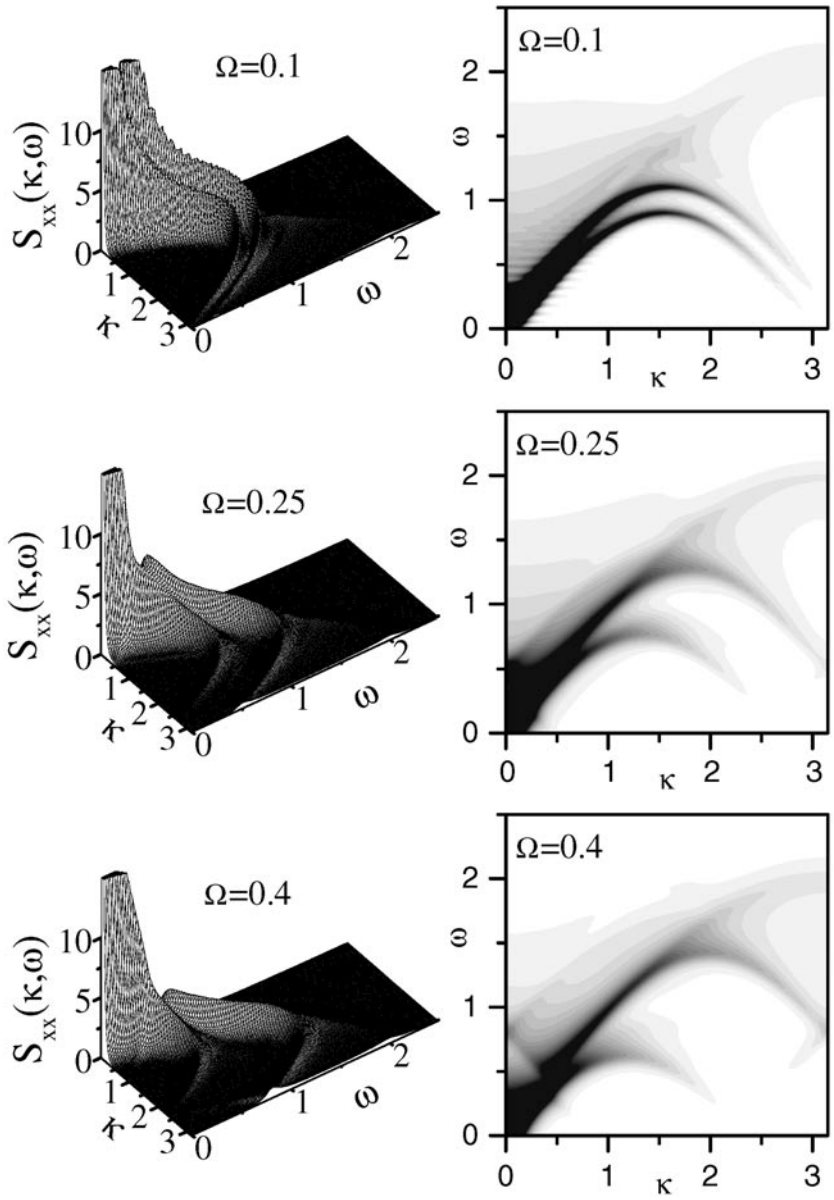

Figure 13. $S_{xx}(\kappa,\omega)$ (3) obtained numerically for the spin chain (1) with $J=-1$, $\delta=0.1$ for different values of the transverse field $\Omega=0.1$, 0.25, 0.4, 0.5, 0.6, 0.75, 0.8, 0.9, 1 at low temperature, $\beta=20$.

isotropic chain without an external field) which is related directly to the neutron scattering spectrum.

Let us start from the case without an external field (at zero temperature). In [8] general arguments for the two-particle excitation (delocalized magnon consisting of two spinons or two free solitons in a bosonized picture of the fermionic theory) continuum with minimum energy 2Δ (Δ is the gap in the energy spectrum) were given. Besides, below the continuum

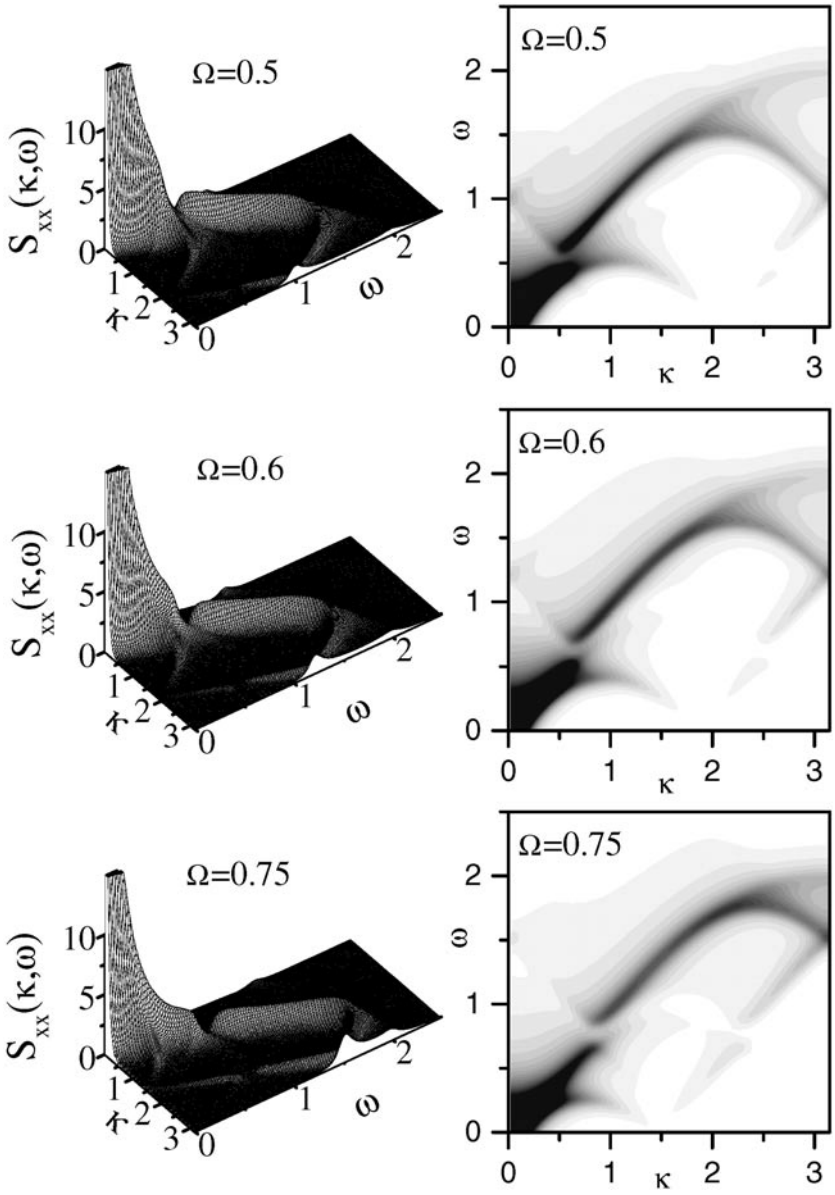

Figure 13. (Continued.)

there is a dispersive one-magnon magnon-like excitation (magnon consisting of two bound spinons or the bound state of two solitons in the bosonized picture) with minimum energy Δ. Numerical computations for $N = 18$ sites [37] confirmed that the dominating feature in $S_{zz}(\kappa, \omega)$ is the one-magnon bound state which is well separated from a continuum of states with larger ω. In contrast, the consideration based on the Hartree–Fock approximation [11] does not predict a separate dispersive excitation. The experimental study of the spin-Peierls phase of $CuGeO_3$ by inelastic neutron scattering by Ain *et al* [3] clearly demonstrated besides a dispersive mode a second gap which separates that mode from the edge of the continuum

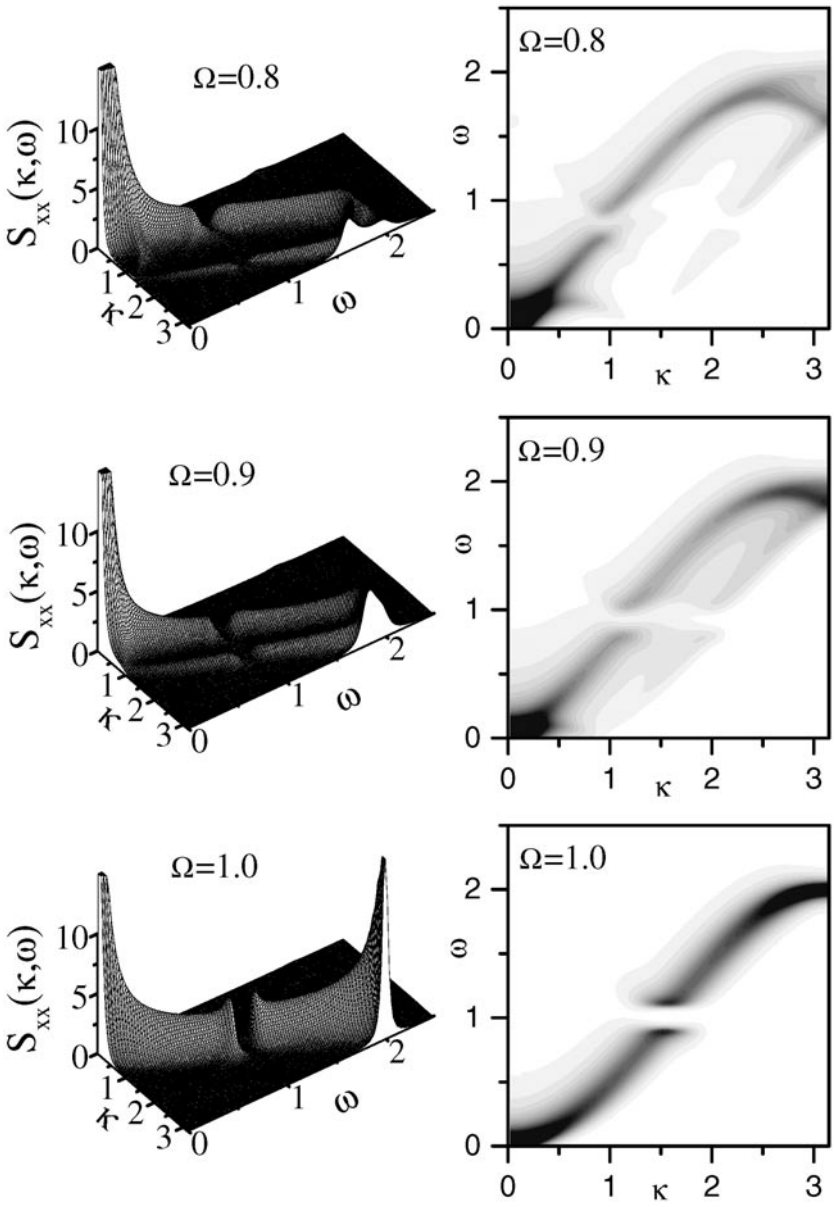

Figure 13. (Continued.)

and which was overlooked in previous experiments because of poor resolution. As one can see from our findings, the XY dimerized chain (without field) does exhibit a gapped two-particle excitation (upper) continuum (figure 8, the panel for $\beta = \infty$ in figure 6) but does not exhibit a gapped dispersive excitation below the continuum. The absence of bound state branches in the XY chain is related to the absence of interactions in the corresponding fermion model. This is quite evident in the case of the z correlations, but less so for the x correlations due to the many-fermion nature of the latter. On the other hand, our results show one more two-particle excitation (lower) continuum which becomes visible as temperature increases (the panels for

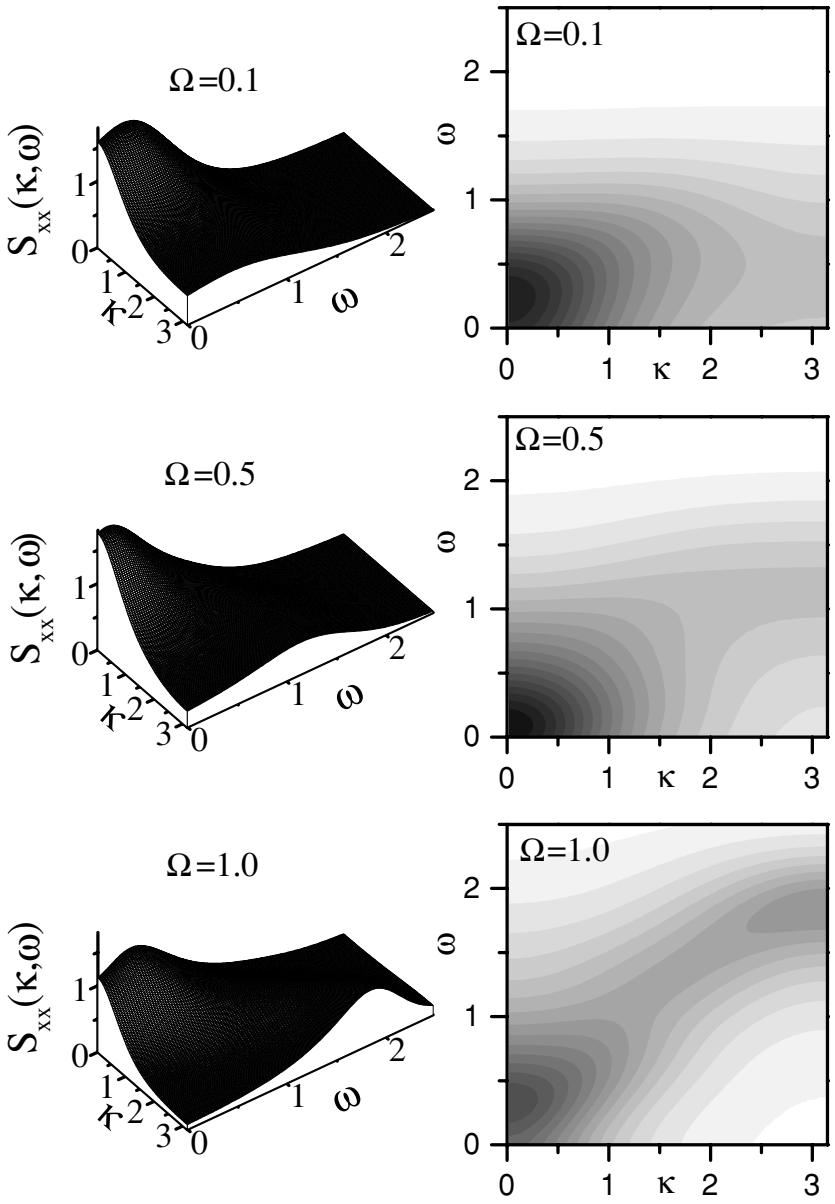

Figure 14. $S_{xx}(\kappa, \omega)$ (3) obtained numerically for the spin chain (1) with $J = -1$, $\delta = 0.1$ for different values of the transverse field $\Omega = 0.1, 0.5, 1$ at high temperature, $\beta = 1$.

$\beta = 20, 5, 1, 0.1, 0.000\,01$ in figure 6). The appearance of that continuum with nonzero temperature (or supercritical field $\Omega > \delta$, see below) follows from the Fermi factors (16), as discussed above.

In the case with an external field (at zero temperature), numerical calculations [37] show that while the field increases the one-magnon bound state moves down to lower ω and as a result the gap closes. The bound two-spinon state (=localized magnon) is destroyed by the field and for larger fields one observes the low-energy two-particle (lower) continuum

(=delocalized magnons). For the XY dimerized chain the lower continuum is absent at zero temperature $\beta = \infty$ until the field exceeds the value $\delta|J|$ at which the gap in the energy spectrum becomes zero (figure 10, figure 9). For larger field (up to the value of J) the two-particle (lower) continuum becomes observable. For nonzero temperatures the lower continuum is visible even for the gapped chain, i.e., when Ω is smaller than $\delta|J|$ as can be seen in figure 6. Moreover, as the temperature becomes high $\beta \to 0$ $S_{zz}(\kappa, \omega)$ becomes field-independent (compare the panels for $\beta = 0.000\,01$ in figures 6 and 7).

To summarize, the XY dimerized chain exhibits some similarities (two two-particle excitation continua) and some differences (no dispersive excitation below the upper continuum) in the dynamic properties in comparison with the Heisenberg chain. Our results give an impression about the changes in the dynamic properties of the XXZ Heisenberg chain as the anisotropy in the exchange interaction increases. Besides, in the presence of exchange interaction anisotropy (as well as of an external field) the dynamic structure factors $S_{zz}(\kappa, \omega)$ and $S_{xx}(\kappa, \omega) = S_{yy}(\kappa, \omega)$ have to be considered separately and we have demonstrated what the differences are in the XY limiting case.

5. Summary

To summarize, we have studied the zz and xx (yy) dynamic structure factors at arbitrary temperatures for the regularly alternating spin-$\frac{1}{2}$ isotropic XY chain in a transverse field. While partial information on the zz structure factor has been available before, the results for the xx structure factor are entirely new. We have compared the low-temperature numerical results for the xx (yy) dynamic structure factor with analytical results available for the zz dynamic structure factor emphasizing the similarities and differences. We have discussed the changes in dynamic properties of the spin chain caused by dimerization at different values of the external (transverse) field demonstrating how those properties depend on microscopic parameters.

The following new results were obtained: (i) the explicit formula for $\left\langle s_j^z(t) s_{j+n}^z \right\rangle$ (5) and a study of the zz time-dependent spin correlations; (ii) $S_{zz}(\kappa, \omega)$ (11) at nonzero temperatures and a discussion of the temperature effects on zz dynamics; (iii) the explicit formula for $\left\langle s_j^x(t) s_{j+n}^x \right\rangle$ (10) (and $S_{xx}(\kappa, \omega)$ (12)) at zero temperature and $\Omega > |J|$; (iv) xx (yy) time-dependent spin correlations and $S_{xx}(\kappa, \omega)$ $(S_{yy}(\kappa, \omega))$ obtained numerically; (v) a comparison with the known results for the dimerized Heisenberg chain.

Acknowledgments

This study was performed within the framework of the STCU project no 1673. The authors are grateful to J Richter (Magdeburg) for useful comments. The paper was partially presented at the Ampere Summer School 'Applications of Magnetic Resonance in Novel Materials', Nafplion, Greece, 3–9 September, 2000. OD thanks the organizers for the support for attending the school. He also acknowledges travel support from *Deutsche Forschungsgemeinschaft* under grant no Kl 645/3-3 (A Klümper) to visit Dortmund University in the summer of 2001.

Appendix

In this appendix we collect some useful formulae from [15] which are used in the discussion of the dynamic structure factors, section 4. The lines $\omega = \epsilon_i(\kappa)$ in the (κ, ω) plane mark (potential) discontinuities in the zero-temperature zz dynamic structure factor. ϵ_0, ϵ_1, ϵ_2 and ϵ_5

are the field-independent boundaries of the continua shown in figure 5, whereas ϵ_1', ϵ_2', ϵ_3 and ϵ_4 are Ω-dependent boundaries resulting from the weight factors (16). They are relevant at $\Omega > \delta$ and visible at low temperature only.

$$\epsilon_0(\kappa) = (1+\delta)\sin\kappa \qquad \kappa_c \leqslant \kappa \leqslant \pi - \kappa_c \qquad \kappa_c = 2\arctan\sqrt{\delta} \tag{A1}$$

$$\epsilon_1(\kappa) = 2\sqrt{\sin^2\frac{\kappa}{2} + \delta^2\cos^2\frac{\kappa}{2}} \tag{A2}$$

$$\epsilon_2(\kappa) = \epsilon_1(\pi - \kappa) \tag{A3}$$

$$\epsilon_1'(\kappa) = \Omega + \Omega^{-1}\sqrt{(\Omega^2\cos\kappa - \sqrt{(\Omega^2-\delta^2)(1-\Omega^2)}\sin\kappa)^2 + \delta^2\sin^2\kappa} \tag{A4}$$

$$\epsilon_2'(\kappa) = \epsilon_1'(\pi - \kappa) \tag{A5}$$

$$\epsilon_3(\kappa) = \left|\Omega - \Omega^{-1}\sqrt{(\Omega^2\cos\kappa - \sqrt{(\Omega^2-\delta^2)(1-\Omega^2)}\sin\kappa)^2 + \delta^2\sin^2\kappa}\right| \tag{A6}$$

$$\epsilon_4(\kappa) = \epsilon_3(\pi - \kappa) \tag{A7}$$

$$\epsilon_5(\kappa) = (1-\delta)\sin\kappa. \tag{A8}$$

References

[1] For a review on the spin-Peierls compound $CuGeO_3$ see, e.g.,
Boucher J P and Regnault L P 1996 *J. Physique* I **6** 1939

[2] For the experimental and theoretical studies on the $s = \frac{1}{2}$ alternating chain compound $(VO)_2P_2O_7$ see, e.g.,
Johnston D C, Johnson J W, Gorshorn D P and Jacobson A J 1987 *Phys. Rev.* B **35** 219
Barnes T and Riera J 1994 *Phys. Rev.* B **50** 6817
Garrett A W, Nagler S E, Tennant D A, Sales B C and Barnes T 1997 *Phys. Rev. Lett.* **79** 745
Tennant D A, Nagler S E, Garrett A W, Barnes T and Torardi C C 1997 *Phys. Rev. Lett.* **78** 4998
Tennant D A, Nagler S E, Barnes T, Garrett A W, Riera J and Sales B C 1997 *Preprint* cond-mat/9708078

[3] Hirota K, Cox D E, Lorenzo J E, Shirane G, Tranquada J M, Hase M, Uchinokura K, Kojima H, Shibuya Y and Tanaka I 1994 *Phys. Rev. Lett.* **73** 736
Nishi M, Fujita O and Akimitsu J 1994 *Phys. Rev.* B **50** 6508
Regnault L P, Ain M, Hennion B, Dhalenne G and Revcolevschi A 1996 *Phys. Rev.* B **53** 5579
Martin M C, Shirane G, Fujii Y, Nishi M, Fujita O, Akimitsu J, Hase M and Uchinokura K 1996 *Phys. Rev.* B **53** R14713
Ain M, Lorenzo J E, Regnault L P, Dhalenne G, Revcolevschi A, Hennion B and Jolicoeur Th 1997 *Phys. Rev. Lett.* **78** 1560

[4] Luther A and Peschel I 1975 *Phys. Rev.* B **12** 3908
Schulz H J 1986 *Phys. Rev.* B **34** 6372

[5] Müller G, Thomas H, Beck H and Bonner J 1981 *Phys. Rev.* B **24** 1429
Müller G, Thomas H, Puga M W and Beck H 1981 *J. Phys. C: Solid State Phys.* **14** 3399

[6] Bonner J C and Blöte H W J 1982 *Phys. Rev.* B **25** 6959

[7] Viswanath V S and Müller G 1994 *The Recursion Method. Application to Many–Body Dynamics* (Berlin: Springer)

[8] Uhrig G S and Schulz H J 1996 *Phys. Rev.* B **54** R9624
Uhrig G S and Schulz H J 1998 *Phys. Rev.* B **58** 2900

[9] Chitra R and Giamarchi T 1997 *Phys. Rev.* B **55** 5816

[10] Starykh O A, Sandvik A W and Singh R R P 1997 *Phys. Rev.* B **55** 14953

[11] Kouzuki A, Kawasaki K and Nakamura K 1999 *Phys. Rev.* B **60** 12874

[12] Lieb E, Schultz T and Mattis D 1961 *Ann. Phys., NY* **16** 407
Katsura S 1962 *Phys. Rev.* **127** 1508

[13] Pincus P 1971 *Solid State Commun.* **9** 1971
Beni G and Pincus P 1972 *J. Chem. Phys.* **57** 3531
Beni G 1973 *J. Chem. Phys.* **58** 3200
[14] Perk J H H, Capel H W, Zuilhof M J and Siskens Th J 1975 *Physica* A **81** 319 and references therein
[15] Taylor J H and Müller G 1985 *Physica* A **130** 1 and references therein
[16] Kennedy T and Lieb E H 1987 *Phys. Rev. Lett.* **59** 1309
[17] Okamoto K and Yasumura K 1990 *J. Phys. Soc. Japan* **59** 993 and references therein
Okamoto K 1992 *Solid State Commun.* **83** 1039
[18] Sil S 1998 *J. Phys.: Condens. Matter* **10** 8851
[19] de Lima J P and Gonçalves L L 1999 *J. Magn. Magn. Mater.* **206** 135
[20] Derzhko O 1999 *Fiz. Nizk. Temp. (Kharkiv)* **25** 575 (1999 *Low Temp. Phys.* **25** 426)
Derzhko O, Richter J and Zaburannyi O 1999 *Phys. Lett.* A **262** 217
Derzhko O, Richter J and Zaburannyi O 2000 *Physica* A **282** 495
Derzhko O, Richter J and Zaburannyi O 2000 *J. Phys.: Condens. Matter* **12** 8661
Derzhko O 2000 *J. Phys. A: Math. Gen.* **33** 8627
[21] Niemeijer Th 1967 *Physica* **36** 377
Katsura S, Horiguchi T and Suzuki M 1970 *Physica* **46** 67
Gersch H A 1970 *Phys. Rev.* B **1** 2270
[22] Brandt U and Jacoby K 1976 *Z. Phys.* B **25** 181
Brandt U and Jacoby K 1977 *Z. Phys.* B **26** 245
[23] Capel H W and Perk J H H 1977 *Physica* A **87** 211
Perk J H H and Capel H W 1977 *Physica* A **89** 265
Perk J H H, Capel H W and Siskens Th J 1977 *Physica* A **89** 304
Perk J H H and Capel H W 1978 *Physica* A **92** 163
[24] Perk J H H and Capel H W 1980 *Physica* A **100** 1
[25] McCoy B M, Barouch E and Abraham D B 1971 *Phys. Rev.* A **4** 2331
[26] Cruz H B and Gonçalves L L 1981 *J. Phys. C: Solid State Phys.* **14** 2785
[27] McCoy B M, Perk J H H and Shrock R E 1983 *Nucl. Phys.* B **220** 35
McCoy B M, Perk J H H and Shrock R E 1983 *Nucl. Phys.* B **220** 269
[28] Müller G and Shrock R E 1984 *Phys. Rev.* B **29** 288
[29] Colomo F, Izergin A G, Korepin V E and Tognetti V 1992 *Phys. Lett.* A **169** 243
Its A R, Izergin A G, Korepin V E and Slavnov N A 1993 *Phys. Rev. Lett.* **70** 1704
Colomo F, Izergin A G and Tognetti V 1997 *J. Phys. A: Math. Gen.* **30** 361
[30] Ilinski K N and Kalinin G V 1996 *Phys. Rev.* E **54** R1017
Ilinskaia A V, Ilinski K N, Kalinin G V, Melezhik V V and Stepanenko A S 1995 *Preprint* cond-mat/9509040
[31] Farias G A and Gonçalves L L 1987 *Phys. Status Solidi* b **139** 315
[32] Stolze J, Nöppert A and Müller G 1995 *Phys. Rev.* B **52** 4319
Stolze J and Vogel M 2000 *Phys. Rev.* B **61** 4026
[33] Fabricius K, Löw U and Stolze J 1997 *Phys. Rev.* B **55** 5833
[34] Sachdev S and Young A P 1997 *Phys. Rev. Lett.* **78** 2220
[35] Derzhko O and Krokhmalskii T 1997 *Phys. Rev.* B **56** 11659
Derzhko O and Krokhmalskii T 1998 *Phys. Status Solidi* b **208** 221
Derzhko O, Krokhmalskii T and Stolze J 2000 *J. Phys. A: Math. Gen.* **33** 3063
[36] Kawasaki K, Maya N, Kouzuki A and Nakamura K 1997 *J. Phys. Soc. Japan* **66** 839
[37] Yu W and Haas S 2000 *Phys. Rev.* B **62** 344
[38] Buzdin A I, Kulić M L and Tugushev V V 1983 *Solid State Commun.* **48** 483
Derzhko O and Krokhmalskii T 2001 *Ferroelectrics* **250** 397
[39] Cavadini N, Henggeler W, Furrer A, Güdel H-U, Krämer K and Mutka H 1999 *Eur. Phys. J.* B **7** 519
Cavadini N, Henggeler W, Furrer A, Güdel H-U, Krämer K and Mutka H 2000 *Physica* B **276–278** 540
[40] Zubarev D N 1971 *Njeravnovjesnaja Statistitchjeskaja Tjermodinamika* (Moscow: Nauka) (in Russian)
(Engl. transl. 1974 *Nonequilibrium Statistical Thermodynamics* (New York: Consultants Bureau))
[41] de Lima J P and Gonçalves L L 2001 *Preprint* cond-mat/0111372
[42] Affleck I 1989 Field theory methods and quantum critical phenomena. *Fields, Strings and Critical Phenomena* ed E Brézin and J Zinn-Justin (Amsterdam: Elsevier) pp 563–640
von Delft J and Schoeller H 1998 *Ann. Phys., Lpz* **7** 225
Rao S and Sen D 2000 *Preprint* cond-mat/0005492